

# Scaling of dynamic thermoelectric harvesting devices in the 1-100 cm<sup>3</sup> range

M. E. Kiziroglou<sup>\*a</sup>, A. Elefsiniotis<sup>b</sup>, N. Kokorakis<sup>b</sup>, S. W. Wright<sup>a</sup>, T. T. Toh<sup>a</sup>, P. D. Mitcheson<sup>a</sup>,  
U. Schmid<sup>c</sup>, Th. Becker<sup>b</sup> and E. M. Yeatman<sup>a</sup>

<sup>a</sup>Department of Electrical and Electronic Engineering, Imperial College London, SW7 2AZ, U.K.

<sup>b</sup>Airbus Group Innovations, Communication and Sensor Department, 81663, Munich, Germany

<sup>c</sup>Institute of Sensor and Actuator Systems, Vienna University of Technology, 1040 Wien, Austria

## ABSTRACT

Aircraft sensors are typically cable powered, imposing a significant weight overhead. The exploitation of temperature variations during flight by a phase change material (PCM) based heat storage thermoelectric energy harvester, as an alternative power source in aeronautical applications, has recently been flight tested. In this work, a scaled-down and a scaled-up prototype are presented. Output energy of 4.1 J per gram of PCM from a typical flight cycle is demonstrated for the scaled-down device, and 3.2 J per gram of PCM for the scaled-up device. The observed performance improvement with scaling down is attributed to the reduction in temperature inhomogeneity inside the PCM. As an application demonstrator for dynamic thermoelectric harvesting devices, the output of a thermoelectric module is used to directly power a microcontroller for the generation of a pulse width modulation signal.

**Keywords:** energy harvesting, thermoelectric, aircraft, sensors, phase change materials, heat storage

## 1. INTRODUCTION

Energy harvesting as the technology of collecting environmental energy that is locally available to power local microsystems such as sensors was proposed at the beginning of the 2000s<sup>1-4</sup>. Fifteen years on, a wealth of different approaches and device implementations have been proposed for exploiting motion, thermoelectric, RF radiation, and light sources. The exploitation of such approaches in useful applications requires that the net available power density is high enough, and that it is available at the desired location, for the desired period of time. In thermoelectric energy harvesting, this translates to the requirement for a temperature difference  $\Delta T$  at the location of installation. Temperature differences are prevalent in industrial environments or in operating engines but they do not necessarily always occur at the required location. This has been a critical limitation in the application of thermoelectric harvesting devices.

For the case of environments where the temperature fluctuates considerably with time, a dynamic thermoelectric harvesting approach has been proposed, using a heat storage unit, implemented by a phase change material (PCM) to induce temperature hysteresis, hence creating a  $\Delta T$  internal to the device. Based on this approach, various prototypes have been reported and the operation and performance of such devices has been analysed<sup>5</sup>. For aircraft monitoring applications, where a considerable temperature cycle occurs during a flight, flight tests have been performed for the characterisation of power generation performance<sup>6</sup>, and another is underway for the demonstration of wireless, harvesting powered strain monitoring during flights<sup>7</sup>. The use of dynamic thermoelectric harvesting has also been considered in countryside environments for applications such as precision agriculture<sup>8</sup>.

The typical volume of the PCM used in prototypes reported so far is in a range around 20 cm<sup>3</sup>. In order to assess the applicability of such devices to different sensor types or application scenarios, it would be very useful to know how the performance of these devices scales with size. Therefore, in this work, two new heat storage thermoelectric harvesting devices are presented: one smaller and one larger than the typical size of devices already reported in the literature. The change of PCM volume is approximately an order of magnitude for both devices. In this way, a first assessment of scalability of this device concept is obtained.

In the following sections, the concept of dynamic thermoelectric harvesting is briefly summarized and then the scaled down and the scaled up prototypes are presented. Their performance is analyzed and the results are discussed and compared with previously reported devices. Finally, as a functional demonstrator, a microcontroller operating while directly powered from the heat storage harvester, using a voltage booster and regulator is presented and conclusions are drawn about the potential use of dynamic thermoelectric harvesting in commercial applications.

## 2. DEVICE CONCEPT

The principle of operation of heat storage thermoelectric harvesting devices has been discussed in detail in previous publications<sup>5,9</sup>. For easy reference, the concept is summarized here, with reference to Figure 1. The device objective is to transform thermal energy from the temperature fluctuation of an environment into electricity. A container with very high heat capacity, the heat storage unit (HSU), is employed alongside a PCM that changes phase within the temperature fluctuation range. The HSU is in thermal contact with the environment only through a thermoelectric generator (TEG). As the environmental temperature fluctuates, heat flows in and out of the HSU through the TEG, resulting in generation of electrical power. The high heat capacity of the HSU and critically, the phase change (i.e. latent) heat of the PCM ensures that a considerable  $\Delta T$  is built up between the inside and outside of the HSU.

The temperature and phase change uniformity inside the HSU can be enhanced by metal thermal bridging, such that any  $\Delta T$  loss across the PCM is minimized. The overall performance of such devices scales with the square of  $\Delta T$ , because both the heat flow and the TEG efficiency scale approximately linearly with  $\Delta T$ . An analysis of the dynamics of operation and performance of this type of devices has been presented in<sup>5</sup> and<sup>10</sup>.

## 3. SCALED DOWN PROTOTYPE

A scaled-down prototype was fabricated based on two different TEG models. The first is the Marlow NL1013T  $13 \times 13 \times 2.4 \text{ mm}^3$  TEG, with an internal electrical resistance of  $7.42 \Omega$  and a thermal resistance of  $16.9 \text{ K/W}$ . This corresponds to a thermal conductivity of  $0.68 \text{ W/mK}$ . The second is the Eureka TEG1-9.1-9.9-0.8/200 with size  $9.1 \times 9.9 \times 2.3 \text{ mm}^3$ , internal electrical resistance  $8.85 \Omega$  and thermal resistance  $30 \text{ K/W}$ . This corresponds to a thermal conductivity of  $0.85 \text{ W/mK}$ . The reference to the value of thermal conductivity, in addition to the thermal resistance, for the two TEGs is given because it is indicative of what could be possible for larger/smaller TEG arrays and the same technology. In other words, the conductivity is independent of TEG dimensions and hence it provides a model-independent comparison of technologies.

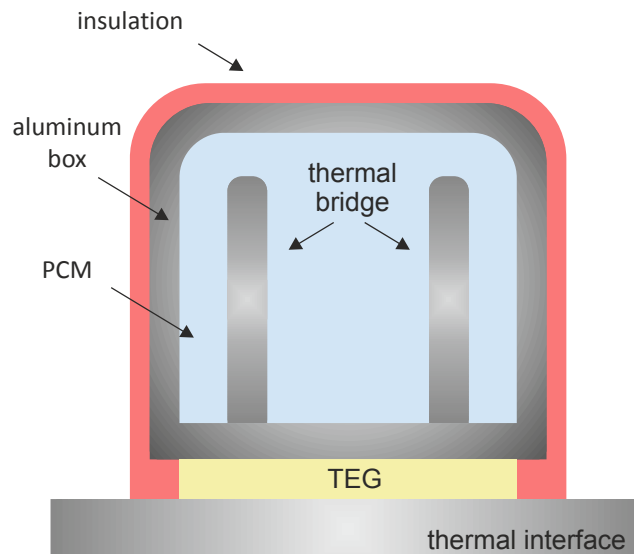


Figure 1. Concept of operation for dynamic thermoelectric harvesting devices.

The heat storage unit comprises an extruded polystyrene (XPS) lid-less box with outer dimensions  $19 \times 19 \times 27$  mm and inner dimensions  $10 \times 10 \times 19$  mm<sup>3</sup> and a 9-fin  $14 \times 14 \times 20$  mm<sup>3</sup> aluminum thermal bridge. The total HSU volume capacity, taking into account the thermal bridge displacement, is 1.8 ml. For the experiments, 1.4 ml of water was used as the PCM. A photograph of the device, with the Marlow TEG installed is shown in Figure 2 (left). The thermal bridge is protruding from the box for illustrative purposes. In Figure 2 (right), a photograph of the device under characterization is shown, featuring the insulated TEG and Pt100 sensor connectors.

The device was characterized in an environmental chamber for various different temperature cycles and with the aircraft environment as an indicative application case. The temperature profiles used were based on available and previously reported data for an aircraft fuselage during flight<sup>6</sup>. The TEG output voltage was monitored across a connected  $7.5 \Omega$  matched load. The temperature and voltage response of the scaled-down prototype with the Marlow TEG installed is presented in Figure 3 (left). The cycle was from  $+22 \text{ }^\circ\text{C}$  to  $-25 \text{ }^\circ\text{C}$  and back, with a temperature change rate of around  $3 \text{ }^\circ\text{C}/\text{min}$ , similar to that observed during typical flight scenarios. A  $\Delta T$  as high as  $15 \text{ }^\circ\text{C}$  is achieved during the cooling down phase, with significant water super-cooling. During the warm up phase, the  $\Delta T$  is substantially smaller, mainly due to the slower change of temperature that is achieved by the environmental chamber. This is because of the large heat flux that is absorbed by the HSU at that point, which affects the HSU outside temperature due to thermal contact limitations. Such limitations do not occur in a flight environment, because there, the heat sink of the HSU is the fuselage of the aircraft. The corresponding power and cumulative energy are presented in Figure 3 (right). The total cumulative energy from a full temperature cycle was 5.8 J. This corresponds to an energy density of 4.14 J per gram of PCM, around 10% lower than the corresponding 4.57 J/g that has been previously reported for a device with 23 g of PCM.

Similar results are obtained using the Eureka TEG, connected to a matched  $8.8 \Omega$  load. The temperature, voltage response, power and cumulative energy are illustrated in Figure 4. The total cumulative energy from a full temperature cycle was 5.5 J, corresponding to an energy density of 3.93 J per gram of PCM.

In both cases, significant super-cooling of the water PCM is observed, which maintains a reduced  $\Delta T$  during its occurrence. However, in the same time it reduces the heat flow preserving it for the phase change stage. Whether super-cooling has a positive or negative effect on the overall output energy depends on the environmental temperature change rate in comparison to the thermal time constant  $RC$  of the device (where  $R$  is the thermal resistance and  $C$  the thermal capacitance of the device). Simulation analysis based on the model introduced in<sup>5</sup> (not shown here), shows that for high rates such as those occurring on aircraft during flight, super-cooling incurs energy loss as high as 6% of the total energy harvested during a full flight cycle. However, for much lower rates (e.g. below  $1 \text{ K}/\text{min}$  for a typical device size) where it is very difficult to achieve an appreciable  $\Delta T$  during non-phase change operation, super-cooling is beneficial because it enables the use of dynamic thermoelectric harvesting in applications with much smaller temperature change rates.

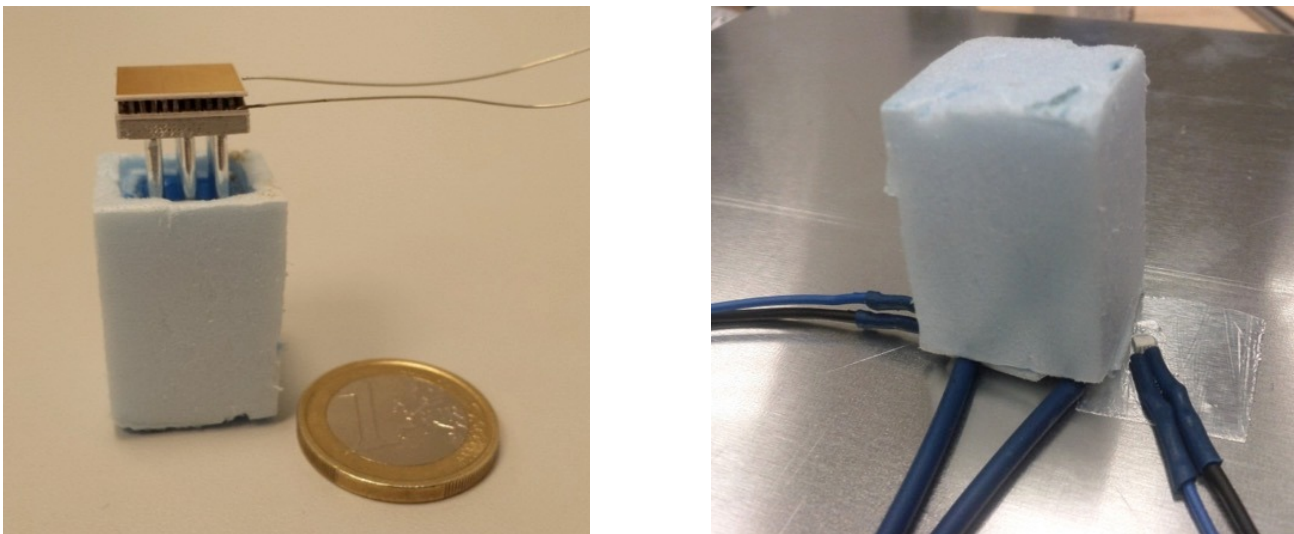


Figure 2. Images of the scaled down prototype. On the left: open device revealing the extruded polystyrene (XPS) heat storage unit, the internal heat sink and the TEG. On the right: Device under test. The middle cable pair is the TEG connectors, while the blue/black cables connect the Pt100 sensors for temperature monitoring.

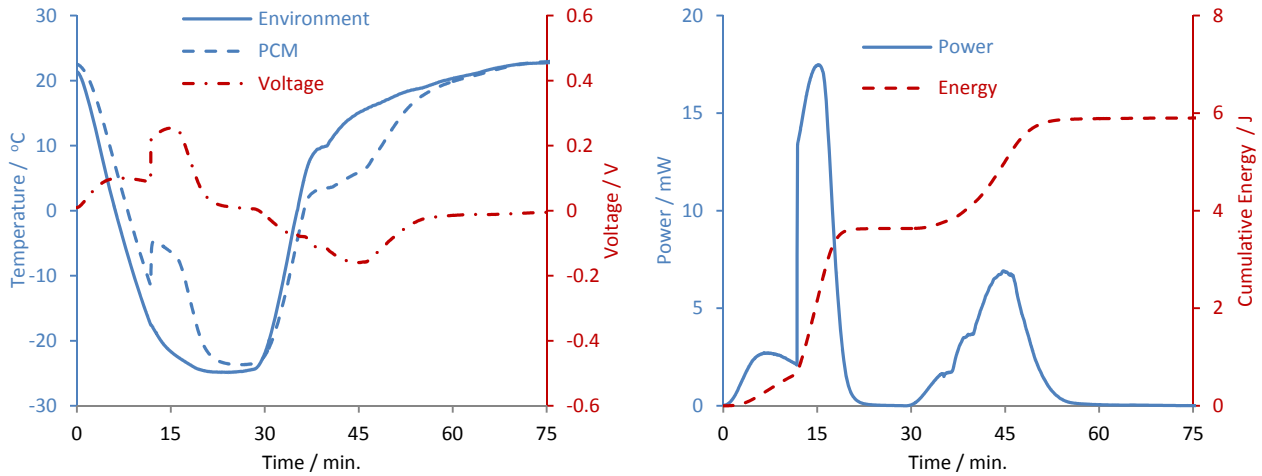


Figure 3. (left) Temperature and output voltage response of the scaled-down prototype (1.4 ml of PCM) during a typical flight temperature cycle using a Marlow TEG and a 7.5  $\Omega$  load resistor. (right) The corresponding power output and energy profiles for this harvester, a total electrical energy of 5.8 J was produced.

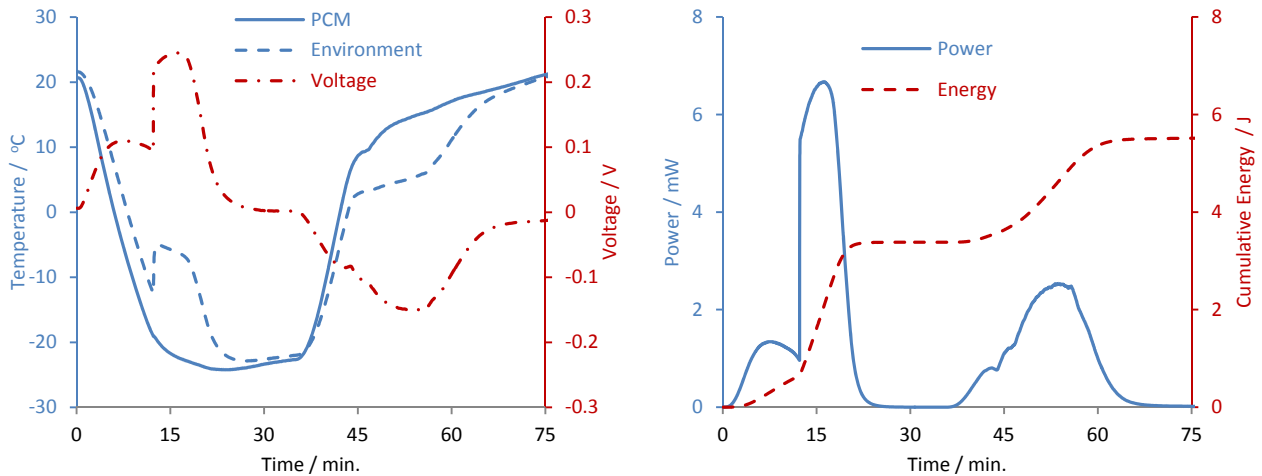


Figure 4. (left) Temperature and output voltage response of the scaled – down prototype (1.4 ml of PCM) during a typical flight temperature cycle using a Eureka TEG and a 9  $\Omega$  load resistor. (right) The corresponding power output and energy profiles for this harvester, a total electrical energy of 5.5 J was produced.

#### 4. SCALED UP PROTOTYPE

For the scaled up prototype a  $40 \times 40 \times 4$  mm<sup>3</sup> Marlow TG12-6L TEG model was used, with an internal electrical resistance of 3.8  $\Omega$  and a thermal resistance of 1.58 K/W. This corresponds to a thermal conductivity of 1.58 W/mK. Again, the reference to the value of thermal conductivity, in addition to the thermal resistance, for the TEG is given for a model-independent comparison of available technologies.

The heat storage unit comprises an extruded polystyrene lid-less box with outer dimensions  $74 \times 135 \times 42$  mm and inner dimensions  $48 \times 108 \times 34$  mm and a size matching multi-fin aluminum thermal bridge. The total HSU volume capacity, taking into account the thermal bridge displacement, is 140 cm<sup>3</sup>. For the experiments, 80 cm<sup>3</sup> of water were used as PCM. A photograph of the device is illustrated in Figure 5. The thermal bridge is protruding from the box for demonstration illustrative purposes. As with the scaled down prototype, the device was characterized in an environmental chamber for various different temperature cycles. The TEG output was connected to a matched 3.8  $\Omega$  load.

The temperature and voltage response of the scaled-up prototype is presented in Figure 6 (left). The cycle was from +22 °C to -20 °C and back, with a temperature change rate of around 4 K/min, similar to the ones presented for the scaled down prototype. The effect of the device heat response to the performance of the environmental chamber is more pronounced, temporarily disrupting the applied temperature cycle. This effect leads to underestimation of the device performance in a real environment. A  $\Delta T$  of 15 °C is achieved both during the cooling down and the warming up phases. Super-cooling is not observed, and this could be attributed to the larger PCM mass, which makes the avoidance of solidification nucleation less likely. However, in order to draw a reliable conclusion about a correlation between super-cooling and device size, further investigation would be required, taking into account the effects of PCM purity, surface to volume ratio and surface texture but also the possibility of vibration – triggered nucleation.

The corresponding power and cumulative energy are presented in Figure 6 (right). The total cumulative energy from a full temperature cycle was 254 J. This corresponds to an energy density of 3.18 J per gram of PCM.

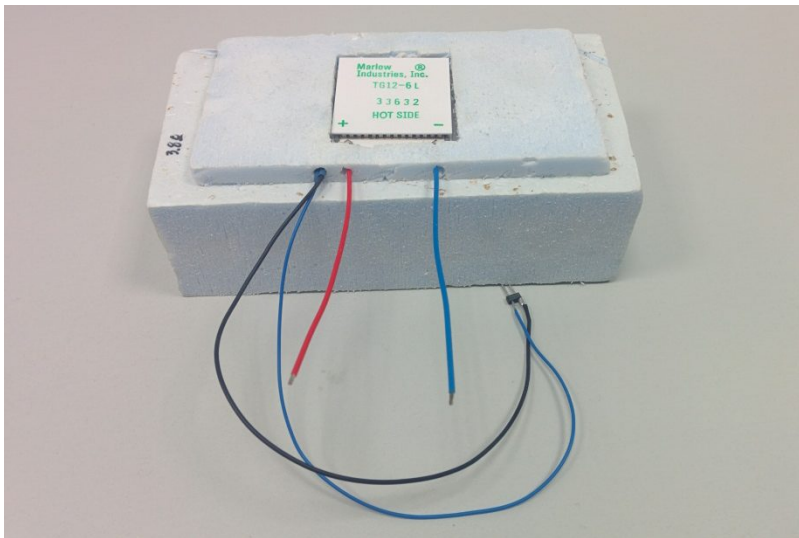


Figure 5. An image of the scaled up prototype. The cable leads for the Marlow TG12-6L TEG and the PT1000 resistance thermometer are also visible. The TEG was placed upside-down for the photo. The side labeled “HOT SIDE” was facing the heat sink for the experiments.

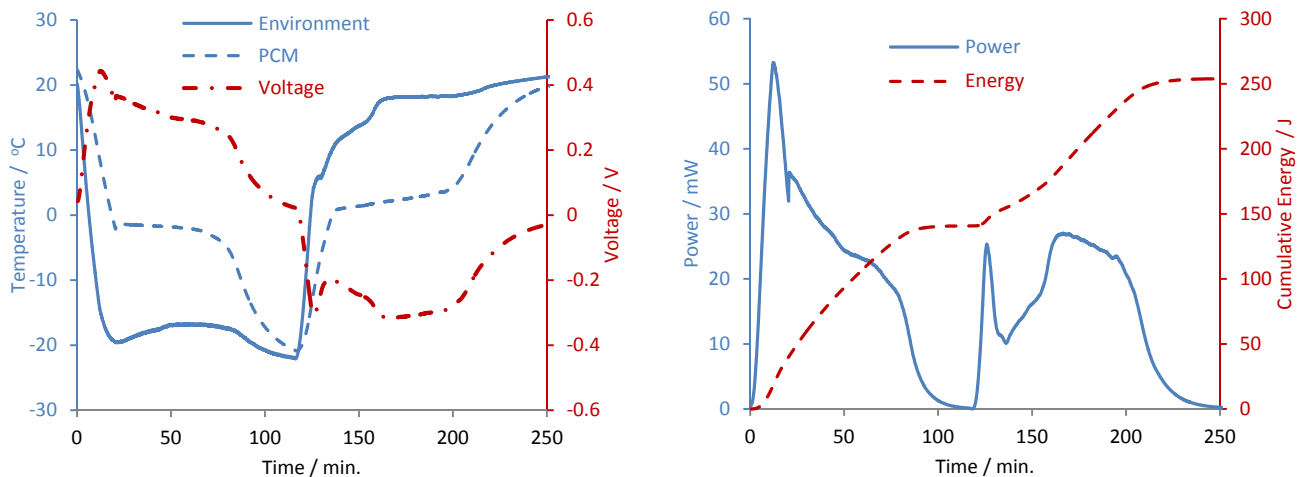


Figure 6. (left) Temperature and output voltage response of the scale-up device (80 ml of PCM) during a typical flight temperature cycle using a Marlow TEG (TG12-6L) and a 3.7 Ω resistor. (right) The corresponding power output and energy profiles for this harvester, a total electrical energy of 254 J was produced.

## 5. DEMONSTRATOR: HEAT STORAGE POWERED MICROCONTROLLER OPERATION

A dynamic thermoelectric energy harvesting device provides an electrical output that is usually stored in a battery or a super-capacitor, either for synchronous or asynchronous use by a sensor node. For this purpose, a power management system is required for rectification, voltage boost, battery charging and regulation, as well as over-charging and over-discharging protection<sup>7</sup>. These stages introduce considerable losses. Therefore, in applications where sensor node activity can depend on power availability, the direct exploitation of the available energy could be preferable. In order to demonstrate the feasibility of such an approach, a battery-less implementation of an electronic system that can operate exclusively on dynamic thermoelectric harvesting power is presented in this section. A block diagram of the system is illustrated in Figure 7. The system uses a dual polarity step-up converter by Linear Technology, namely the LTC3109 integrated circuit which is intended for use with TEG sources. The output of the converter directly supplies power to a Silicon Labs EFM32 microcontroller which is programmed to generate a 10 Hz pulse width modulation signal, in order to demonstrate successful active operation. Experimental results showing a stable 3.3 V output from the LTC3109 when supplied with a 30 mV output from the scaled-down harvester, and the PWM signal generated by the microcontroller are presented in Figure 8.

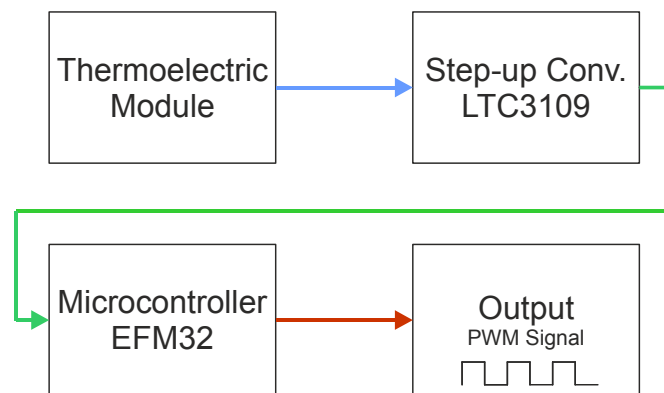


Figure 7. Schematic diagram of the microcontroller demonstrator system.

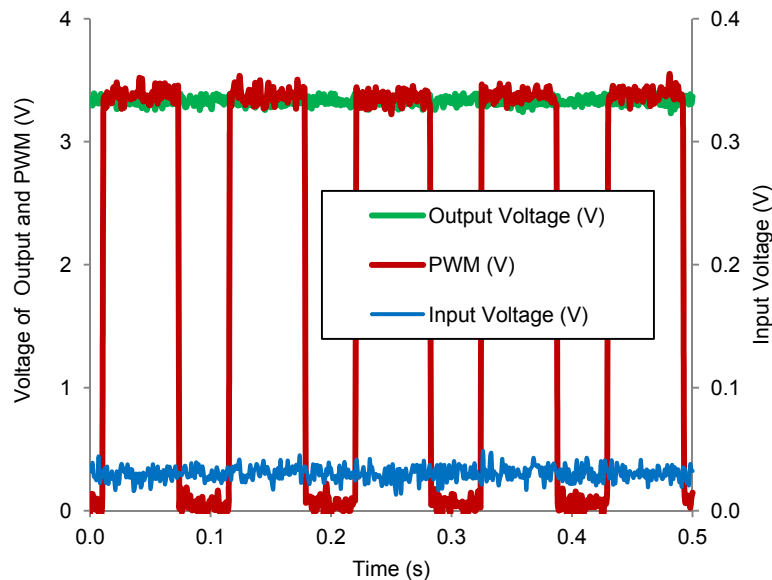


Figure 8. Pulse width modulation operation of the microcontroller, powered directly from the heat storage harvester. The observed noise originates from the measurement equipment used.

## 6. CONCLUSION

A summary of the main features and energy density demonstrated by the two scaled devices is given in Table 1. For comparison, three other implementations of dynamic thermoelectric harvesting are also included. The performance in general depends significantly on the materials used and the design of the heat storage unit, including the thermal bridge and the insulation. Yet, all prototypes yield an energy density between 3 J and 5 J per gram of PCM. The corresponding maximum theoretically achievable energy density for the particular temperature cycle used and the currently available TEGs ( $ZT \sim 0.7$ ), is 10 J per gram of PCM<sup>5</sup>.

While no increasing or decreasing trend can yet be identified for the energy density as a function of size, it can be concluded that these devices can provide considerable power, at least in the 1 – 100 cm<sup>3</sup> range. An instructive indication of power availability can be found in the comparison of performance, in terms of J per PCM volume, against state of the art non-rechargeable batteries. The output of the dynamic thermoelectric harvesting prototypes will reach the energy density of an alkaline battery (1.8 kJ/ml) after 400-650 cycles of operation and a lithium one (4.32 kJ/ml) after 1000-1500 cycles. Performance degradation is not expected due to the solid state nature of the TEGs and the passive chemical nature of the PCM used, contrary to chemical energy storage media like batteries.

With regard to the observation and discussion of the super-cooling effect, it is expected that applications with fast temperature sweep rates would benefit from suppression of super cooling. In contrast, applications with very slow temperature sweep rates could benefit from (or, under certain conditions, even rely on) super-cooling. In order to distinguish between the two cases, the PCM volume, and hence the device size should be taken into account. Particularly the indication that super-cooling in smaller devices could be both more likely and favourable is important for applications with small device sizes and slow temperature fluctuations.

Further study on the scaling of dynamic thermoelectric harvesting devices could involve a combined multi-parameter analysis and numerical simulation. Such a study is expected to identify new methods and device designs, optimized for particular use cases.

Table 1. Comparison of energy density among different dynamic harvester implementations.

Organisation/Year	Size/cm <sup>3</sup>	TEG	Energy J	Energy Density J / cm <sup>3</sup> (PCM)	Energy Density J / cm <sup>3</sup> (device)
EADS / 2008 <sup>11</sup>	24 plus Insulation	4 x Eureka TEG1-9.1-9.9-0.8/200	35	3.5	1.5 (without insulation)
LAAS-CNRS / 2008 <sup>12</sup>	-	Micropelt MPGD602	34	2.8	-
Imperial / 2014 <sup>5</sup>	78	2 x Marlow TG12-2-5	105	4.57	1.3
Imperial and EADS/2015 (This paper, scale down 1)	9.7	Marlow NL1013T	5.8	4.14	0.6
Imperial and EADS/2015 (This paper, scale down 2)	9.7	Eureka TEG1-9.1-9.9-0.8/200	5.5	3.93	0.6
Imperial and EADS/2015 (This paper, scale up)	420	Marlow TG12-6L	254	3.18	0.6

## REFERENCES

- [1] H. A. Sodano, D. J. Inman, and G. Park, "Comparison of piezoelectric energy harvesting devices for recharging batteries," *Journal of Intelligent Material Systems and Structures*, 16(10), 799-807 (2005).
- [2] P. D. Mitcheson, T. C. Green, E. M. Yeatman *et al.*, "Architectures for vibration-driven micropower generators," *Microelectromechanical Systems, Journal of*, 13(3), 429-440 (2004).
- [3] P. Glynne-Jones, M. J. Tudor, S. P. Beeby *et al.*, "An electromagnetic, vibration-powered generator for intelligent sensor systems," *Sensors and Actuators A: Physical*, 110(1-3), 344-349 (2004).
- [4] N. S. Shenck, and J. A. Paradiso, "Energy scavenging with shoe-mounted piezoelectrics," *IEEE Micro*, 21(3), 30-42 (2001).
- [5] M. E. Kiziroglou, S. W. Wright, T. T. Toh *et al.*, "Design and Fabrication of Heat Storage Thermoelectric Harvesting Devices," *Industrial Electronics, IEEE Transactions on*, 61(1), 302-309 (2014).
- [6] A. Elefsiniotis, D. Samson, T. Becker *et al.*, "Investigation of the Performance of Thermoelectric Energy Harvesters Under Real Flight Conditions," *Journal of Electronic Materials*, 42(7), 2301-2305 (2013).
- [7] T. T. Toh, S. W. Wright, M. E. Kiziroglou *et al.*, "A dual polarity, cold-starting interface circuit for heat storage energy harvesters," *Sensors and Actuators A: Physical*, 211(0), 38-44 (2014).
- [8] A. A. Papachristou, M. E. Kiziroglou, L. Petrou, S. Koundouras and A. A. Hatzopoulos, Viability of Thermoelectric Energy Harvesting for Precision Agriculture Sensor Nodes, 8th Jordanian International Electrical and Electronics Engineering Conference, Jordan, 16-18 Apr. 2013
- [9] T. Becker, A. Elefsiniotis, and M. E. Kiziroglou, "Thermoelectric Energy Harvesting in Aircraft," in *Micro Energy Harvesting*, D. Briand, S. Roundy, and E. Yeatman, Eds., ed: Wiley, 2014
- [10] M. Kiziroglou, A. Elefsiniotis, S. Wright *et al.*, "Performance of phase change materials for heat storage thermoelectric harvesting," *Applied Physics Letters*, 103(19), 193902 (2013).
- [11] D. Samson, T. Otterpohl, M. Kluge, U. Schmid and Th. Becker, Aircraft-Specific Thermoelectric Generator Module. *Journal of Electronic Materials*, 39(9), pp. 2092-2095, 2009.
- [12] N. Bailly, J.-M. Dilhac, C. Escriba *et al.*, "Energy scavenging based on transient thermal gradients: Applications to structural health monitoring of aircraft." 205-208 (2008).